

Collins asymmetries in inclusive charged KK and $K\pi$ pairs produced in e^+e^- annihilation

J. P. Lees,¹ V. Poireau,¹ V. Tisserand,¹ E. Grauges,² A. Palano^{ab,3} G. Eigen,⁴ B. Stugu,⁴ D. N. Brown,⁵ L. T. Kerth,⁵ Yu. G. Kolomensky,⁵ M. J. Lee,⁵ G. Lynch,⁵ H. Koch,⁶ T. Schroeder,⁶ C. Hearty,⁷ T. S. Mattison,⁷ J. A. McKenna,⁷ R. Y. So,⁷ A. Khan,⁸ V. E. Blinov^{abc,9} A. R. Buzykaev^{a,9} V. P. Druzhinin^{ab,9} V. B. Golubev^{ab,9} E. A. Kravchenko^{ab,9} A. P. Onuchin^{abc,9} S. I. Serednyakov^{ab,9} Yu. I. Skovpen^{ab,9} E. P. Solodov^{ab,9} K. Yu. Todyshev^{ab,9} A. J. Lankford,¹⁰ B. Dey,¹¹ J. W. Gary,¹¹ O. Long,¹¹ M. Franco Sevilla,¹² T. M. Hong,¹² D. Kovalskiy,¹² J. D. Richman,¹² C. A. West,¹² A. M. Eisner,¹³ W. S. Lockman,¹³ W. Panduro Vazquez,¹³ B. A. Schumm,¹³ A. Seiden,¹³ D. S. Chao,¹⁴ C. H. Cheng,¹⁴ B. Echenard,¹⁴ K. T. Flood,¹⁴ D. G. Hitlin,¹⁴ T. S. Miyashita,¹⁴ P. Ongmongkolkul,¹⁴ F. C. Porter,¹⁴ M. Röhrken,¹⁴ R. Andreassen,¹⁵ Z. Huard,¹⁵ B. T. Meadows,¹⁵ B. G. Pushpawela,¹⁵ M. D. Sokoloff,¹⁵ L. Sun,¹⁵ P. C. Bloom,¹⁶ W. T. Ford,¹⁶ A. Gaz,¹⁶ J. G. Smith,¹⁶ S. R. Wagner,¹⁶ R. Ayad,^{17,*} W. H. Toki,¹⁷ B. Spaan,¹⁸ D. Bernard,¹⁹ M. Verderi,¹⁹ S. Playfer,²⁰ D. Bettoni^{a,21} C. Bozzi^{a,21} R. Calabrese^{ab,21} G. Cibinetto^{ab,21} E. Fioravanti^{ab,21} I. Garzia^{ab,21} E. Luppi^{ab,21} L. Piemontese^{a,21} V. Santoro^{a,21} A. Calcaterra,²² R. de Sangro,²² G. Finocchiaro,²² S. Martellotti,²² P. Patteri,²² I. M. Peruzzi,^{22,†} M. Piccolo,²² A. Zallo,²² R. Contri^{ab,23} M. R. Monge^{ab,23} S. Passaggio^{a,23} C. Patrignani^{ab,23} B. Bhuyan,²⁴ V. Prasad,²⁴ A. Adametz,²⁵ U. Uwer,²⁵ H. M. Lacker,²⁶ U. Mallik,²⁷ C. Chen,²⁸ J. Cochran,²⁸ S. Prell,²⁸ H. Ahmed,²⁹ A. V. Gritsan,³⁰ N. Arnaud,³¹ M. Davier,³¹ D. Derkach,³¹ G. Grosdidier,³¹ F. Le Diberder,³¹ A. M. Lutz,³¹ B. Malaescu,^{31,‡} P. Roudeau,³¹ A. Stocchi,³¹ G. Wormser,³¹ D. J. Lange,³² D. M. Wright,³² J. P. Coleman,³³ J. R. Fry,³³ E. Gabathuler,³³ D. E. Hutchcroft,³³ D. J. Payne,³³ C. Touramanis,³³ A. J. Bevan,³⁴ F. Di Lodovico,³⁴ R. Sacco,³⁴ G. Cowan,³⁵ D. N. Brown,³⁶ C. L. Davis,³⁶ A. G. Denig,³⁷ M. Fritsch,³⁷ W. Gradl,³⁷ K. Griessinger,³⁷ A. Hafner,³⁷ K. R. Schubert,³⁷ R. J. Barlow,^{38,§} G. D. Lafferty,³⁸ R. Cenci,³⁹ B. Hamilton,³⁹ A. Jawahery,³⁹ D. A. Roberts,³⁹ R. Cowan,⁴⁰ R. Cheaib,⁴¹ P. M. Patel,^{41,¶} S. H. Robertson,⁴¹ N. Neri^{a,42} F. Palombo^{ab,42} L. Cremaldi,⁴³ R. Godang,^{43,**} D. J. Summers,⁴³ M. Simard,⁴⁴ P. Taras,⁴⁴ G. De Nardo^{ab,45} G. Onorato^{ab,45} C. Sciacca^{ab,45} G. Raven,⁴⁶ C. P. Jessop,⁴⁷ J. M. LoSecco,⁴⁷ K. Honscheid,⁴⁸ R. Kass,⁴⁸ M. Margoni^{ab,49} M. Morandin^{a,49} M. Posocco^{a,49} M. Rotondo^{a,49} G. Simi^{ab,49} F. Simonetto^{ab,49} R. Stroili^{ab,49} S. Akar,⁵⁰ E. Ben-Haim,⁵⁰ M. Bomben,⁵⁰ G. R. Bonneaud,⁵⁰ H. Briand,⁵⁰ G. Calderini,⁵⁰ J. Chauveau,⁵⁰ Ph. Leruste,⁵⁰ G. Marchiori,⁵⁰ J. Ocariz,⁵⁰ M. Biasini^{ab,51} E. Manoni^{a,51} A. Rossi^{a,51} C. Angelini^{ab,52} G. Batignani^{ab,52} S. Bettarini^{ab,52} M. Carpinelli^{ab,52,††} G. Casarosa^{ab,52} M. Chrzaszcz^{a,52} F. Forti^{ab,52} M. A. Giorgi^{ab,52} A. Lusiani^{ac,52} B. Oberhof^{ab,52} E. Paoloni^{ab,52} M. Rama^{a,52} G. Rizzo^{ab,52} J. J. Walsh^{a,52} D. Lopes Pegna,⁵³ J. Olsen,⁵³ A. J. S. Smith,⁵³ F. Anulli^{a,54} R. Faccini^{ab,54} F. Ferrarotto^{a,54} F. Ferroni^{ab,54} M. Gaspero^{ab,54} A. Pilloni^{ab,54} G. Piredda^{a,54} C. Büniger,⁵⁵ S. Dittrich,⁵⁵ O. Grünberg,⁵⁵ M. Hess,⁵⁵ T. Leddig,⁵⁵ C. Voß,⁵⁵ R. Waldi,⁵⁵ T. Adye,⁵⁶ E. O. Olaiya,⁵⁶ F. F. Wilson,⁵⁶ S. Emery,⁵⁷ G. Vasseur,⁵⁷ D. Aston,⁵⁸ D. J. Bard,⁵⁸ C. Cartaro,⁵⁸ M. R. Convery,⁵⁸ J. Dorfan,⁵⁸ G. P. Dubois-Felsmann,⁵⁸ W. Dunwoodie,⁵⁸ M. Ebert,⁵⁸ R. C. Field,⁵⁸ B. G. Fulsom,⁵⁸ M. T. Graham,⁵⁸ C. Hast,⁵⁸ W. R. Innes,⁵⁸ P. Kim,⁵⁸ D. W. G. S. Leith,⁵⁸ S. Luitz,⁵⁸ V. Luth,⁵⁸ D. B. MacFarlane,⁵⁸ D. R. Müller,⁵⁸ H. Neal,⁵⁸ T. Pulliam,⁵⁸ B. N. Ratcliff,⁵⁸ A. Roodman,⁵⁸ R. H. Schindler,⁵⁸ A. Snyder,⁵⁸ D. Su,⁵⁸ M. K. Sullivan,⁵⁸ J. Va'vra,⁵⁸ W. J. Wisniewski,⁵⁸ H. W. Wulsin,⁵⁸ M. V. Purohit,⁵⁹ J. R. Wilson,⁵⁹ A. Randle-Conde,⁶⁰ S. J. Sekula,⁶⁰ M. Bellis,⁶¹ P. R. Burchat,⁶¹ E. M. T. Puccio,⁶¹ M. S. Alam,⁶² J. A. Ernst,⁶² R. Gorodeisky,⁶³ N. Guttman,⁶³ D. R. Peimer,⁶³ A. Soffer,⁶³ S. M. Spanier,⁶⁴ J. L. Ritchie,⁶⁵ R. F. Schwitters,⁶⁵ J. M. Izen,⁶⁶ X. C. Lou,⁶⁶ F. Bianchi^{ab,67} F. De Mori^{ab,67} A. Filippi^{a,67} D. Gamba^{ab,67} L. Lancieri^{ab,68} L. Vitale^{ab,68} F. Martinez-Vidal,⁶⁹ A. Oyanguren,⁶⁹ J. Albert,⁷⁰ Sw. Banerjee,⁷⁰ A. Beaulieu,⁷⁰ F. U. Bernlochner,⁷⁰ H. H. F. Choi,⁷⁰ G. J. King,⁷⁰ R. Kowalewski,⁷⁰ M. J. Lewczuk,⁷⁰ T. Lueck,⁷⁰ I. M. Nugent,⁷⁰ J. M. Roney,⁷⁰ R. J. Sobie,⁷⁰ N. Tasneem,⁷⁰ T. J. Gershon,⁷¹ P. F. Harrison,⁷¹ T. E. Latham,⁷¹ H. R. Band,⁷² S. Dasu,⁷² Y. Pan,⁷² R. Prepost,⁷² and S. L. Wu⁷²

(The BABAR Collaboration)

¹Laboratoire d'Annecy-le-Vieux de Physique des Particules (LAPP),
Université de Savoie, CNRS/IN2P3, F-74941 Annecy-Le-Vieux, France

²Universitat de Barcelona, Facultat de Física, Departament ECM, E-08028 Barcelona, Spain

- ³INFN Sezione di Bari^a; Dipartimento di Fisica, Università di Bari^b, I-70126 Bari, Italy
⁴University of Bergen, Institute of Physics, N-5007 Bergen, Norway
- ⁵Lawrence Berkeley National Laboratory and University of California, Berkeley, California 94720, USA
- ⁶Ruhr Universität Bochum, Institut für Experimentalphysik 1, D-44780 Bochum, Germany
- ⁷University of British Columbia, Vancouver, British Columbia, Canada V6T 1Z1
- ⁸Brunel University, Uxbridge, Middlesex UB8 3PH, United Kingdom
- ⁹Budker Institute of Nuclear Physics SB RAS, Novosibirsk 630090^a,
 Novosibirsk State University, Novosibirsk 630090^b,
 Novosibirsk State Technical University, Novosibirsk 630092^c, Russia
- ¹⁰University of California at Irvine, Irvine, California 92697, USA
- ¹¹University of California at Riverside, Riverside, California 92521, USA
- ¹²University of California at Santa Barbara, Santa Barbara, California 93106, USA
- ¹³University of California at Santa Cruz, Institute for Particle Physics, Santa Cruz, California 95064, USA
- ¹⁴California Institute of Technology, Pasadena, California 91125, USA
- ¹⁵University of Cincinnati, Cincinnati, Ohio 45221, USA
- ¹⁶University of Colorado, Boulder, Colorado 80309, USA
- ¹⁷Colorado State University, Fort Collins, Colorado 80523, USA
- ¹⁸Technische Universität Dortmund, Fakultät Physik, D-44221 Dortmund, Germany
- ¹⁹Laboratoire Leprince-Ringuet, Ecole Polytechnique, CNRS/IN2P3, F-91128 Palaiseau, France
- ²⁰University of Edinburgh, Edinburgh EH9 3JZ, United Kingdom
- ²¹INFN Sezione di Ferrara^a; Dipartimento di Fisica e Scienze della Terra, Università di Ferrara^b, I-44122 Ferrara, Italy
- ²²INFN Laboratori Nazionali di Frascati, I-00044 Frascati, Italy
- ²³INFN Sezione di Genova^a; Dipartimento di Fisica, Università di Genova^b, I-16146 Genova, Italy
- ²⁴Indian Institute of Technology Guwahati, Guwahati, Assam, 781 039, India
- ²⁵Universität Heidelberg, Physikalisches Institut, D-69120 Heidelberg, Germany
- ²⁶Humboldt-Universität zu Berlin, Institut für Physik, D-12489 Berlin, Germany
- ²⁷University of Iowa, Iowa City, Iowa 52242, USA
- ²⁸Iowa State University, Ames, Iowa 50011-3160, USA
- ²⁹Physics Department, Jazan University, Jazan 22822, Kingdom of Saudi Arabia
- ³⁰Johns Hopkins University, Baltimore, Maryland 21218, USA
- ³¹Laboratoire de l'Accélérateur Linéaire, IN2P3/CNRS et Université Paris-Sud 11,
 Centre Scientifique d'Orsay, F-91898 Orsay Cedex, France
- ³²Lawrence Livermore National Laboratory, Livermore, California 94550, USA
- ³³University of Liverpool, Liverpool L69 7ZE, United Kingdom
- ³⁴Queen Mary, University of London, London, E1 4NS, United Kingdom
- ³⁵University of London, Royal Holloway and Bedford New College, Egham, Surrey TW20 0EX, United Kingdom
- ³⁶University of Louisville, Louisville, Kentucky 40292, USA
- ³⁷Johannes Gutenberg-Universität Mainz, Institut für Kernphysik, D-55099 Mainz, Germany
- ³⁸University of Manchester, Manchester M13 9PL, United Kingdom
- ³⁹University of Maryland, College Park, Maryland 20742, USA
- ⁴⁰Massachusetts Institute of Technology, Laboratory for Nuclear Science, Cambridge, Massachusetts 02139, USA
- ⁴¹McGill University, Montréal, Québec, Canada H3A 2T8
- ⁴²INFN Sezione di Milano^a; Dipartimento di Fisica, Università di Milano^b, I-20133 Milano, Italy
- ⁴³University of Mississippi, University, Mississippi 38677, USA
- ⁴⁴Université de Montréal, Physique des Particules, Montréal, Québec, Canada H3C 3J7
- ⁴⁵INFN Sezione di Napoli^a; Dipartimento di Scienze Fisiche,
 Università di Napoli Federico II^b, I-80126 Napoli, Italy
- ⁴⁶NIKHEF, National Institute for Nuclear Physics and High Energy Physics, NL-1009 DB Amsterdam, The Netherlands
- ⁴⁷University of Notre Dame, Notre Dame, Indiana 46556, USA
- ⁴⁸Ohio State University, Columbus, Ohio 43210, USA
- ⁴⁹INFN Sezione di Padova^a; Dipartimento di Fisica, Università di Padova^b, I-35131 Padova, Italy
- ⁵⁰Laboratoire de Physique Nucléaire et de Hautes Energies,
 IN2P3/CNRS, Université Pierre et Marie Curie-Paris6,
 Université Denis Diderot-Paris7, F-75252 Paris, France
- ⁵¹INFN Sezione di Perugia^a; Dipartimento di Fisica, Università di Perugia^b, I-06123 Perugia, Italy
- ⁵²INFN Sezione di Pisa^a; Dipartimento di Fisica,
 Università di Pisa^b; Scuola Normale Superiore di Pisa^c, I-56127 Pisa, Italy
- ⁵³Princeton University, Princeton, New Jersey 08544, USA
- ⁵⁴INFN Sezione di Roma^a; Dipartimento di Fisica,
 Università di Roma La Sapienza^b, I-00185 Roma, Italy
- ⁵⁵Universität Rostock, D-18051 Rostock, Germany
- ⁵⁶Rutherford Appleton Laboratory, Chilton, Didcot, Oxon, OX11 0QX, United Kingdom
- ⁵⁷CEA, Irfu, SPP, Centre de Saclay, F-91191 Gif-sur-Yvette, France
- ⁵⁸SLAC National Accelerator Laboratory, Stanford, California 94309 USA

⁵⁹University of South Carolina, Columbia, South Carolina 29208, USA

⁶⁰Southern Methodist University, Dallas, Texas 75275, USA

⁶¹Stanford University, Stanford, California 94305-4060, USA

⁶²State University of New York, Albany, New York 12222, USA

⁶³Tel Aviv University, School of Physics and Astronomy, Tel Aviv, 69978, Israel

⁶⁴University of Tennessee, Knoxville, Tennessee 37996, USA

⁶⁵University of Texas at Austin, Austin, Texas 78712, USA

⁶⁶University of Texas at Dallas, Richardson, Texas 75083, USA

⁶⁷INFN Sezione di Torino^a; Dipartimento di Fisica, Università di Torino^b, I-10125 Torino, Italy

⁶⁸INFN Sezione di Trieste^a; Dipartimento di Fisica, Università di Trieste^b, I-34127 Trieste, Italy

⁶⁹IFIC, Universitat de Valencia-CSIC, E-46071 Valencia, Spain

⁷⁰University of Victoria, Victoria, British Columbia, Canada V8W 3P6

⁷¹Department of Physics, University of Warwick, Coventry CV4 7AL, United Kingdom

⁷²University of Wisconsin, Madison, Wisconsin 53706, USA

We present measurements of Collins asymmetries in the inclusive process $e^+e^- \rightarrow h_1 h_2 X$, $h_1 h_2 = KK, K\pi, \pi\pi$, at the center-of-mass energy of 10.6 GeV, using a data sample of 468 fb^{-1} collected by the BABAR experiment at the PEP-II B factory at SLAC National Accelerator Center. Considering hadrons in opposite thrust hemispheres of hadronic events, we observe clear azimuthal asymmetries in the ratio of unlike-sign to like-sign, and unlike-sign to all charged $h_1 h_2$ pairs, which increase with hadron energies. The $K\pi$ asymmetries are similar to those measured for the $\pi\pi$ pairs, whereas those measured for high-energy KK pairs are, in general, larger.

PACS numbers: 13.66.Bc, 13.87.Fh, 13.88.+e, 14.65.-q

The Collins effect [1] relates the transverse spin component of a fragmenting quark to the azimuthal distribution of final state hadrons about its flight direction. The chiral-odd, transverse momentum-dependent Collins fragmentation function (FF) provides a unique probe of quantum chromodynamics (QCD), such as factorization and evolution with the energy scale Q^2 [2–5].

Additional interest has been sparked by the observation of azimuthal asymmetries for pions and kaons in semi-inclusive deep inelastic scattering experiments (SIDIS) [6–10]. These are sensitive to the product of a Collins FF and a chiral-odd transversity parton distribution function (PDF), one of the three fundamental PDFs needed to describe the spin content of the nucleon. Although these observations require nonzero Collins FFs, independent direct measurements of one of these chiral-odd functions are needed to determine each of them.

In e^+e^- annihilation, one can measure the product of two Collins FFs, and detailed measurements have been made for pairs of charged pions [11–13]. No measurements are available for $K\pi$ and KK pairs, which are sensitive to different quark-flavor combinations, in particular the contribution of the strange quark. Such measurements could be combined with SIDIS data to simultaneously determine the Collins FFs and transversity PDF for up, down, and strange quarks [14–19].

In this paper, we report the measurement of the Collins effect (or Collins asymmetry) for inclusive production of hadron pairs in the process $e^+e^- \rightarrow q\bar{q} \rightarrow h_1 h_2 X$, where $h_{1,2} = K^\pm$ or π^\pm , q stands for light quarks u or d or s , and X for any combination of additional hadrons.

The probability that a transversely polarized quark (q^\uparrow) with momentum direction $\hat{\mathbf{k}}$ and spin \mathbf{S}_q fragments

into a hadron h carrying zero intrinsic spin with momentum \mathbf{P}_h , is defined in terms of unpolarized D_1^q and Collins $H_1^{\perp q}$ fragmentation functions [20]:

$$D_h^{q\uparrow}(z, \mathbf{P}_{hT}) = D_1^q(z, P_{hT}^2) + H_1^{\perp q}(z, P_{hT}^2) \frac{(\hat{\mathbf{k}} \times \mathbf{P}_{hT}) \cdot \mathbf{S}_q}{zM_h}, \quad (1)$$

where M_h , \mathbf{P}_{hT} , and $z = 2E_h/\sqrt{s}$ are the hadron mass, momentum transverse to $\hat{\mathbf{k}}$, and fractional energy, respectively, with E_h its total energy and \sqrt{s} the e^+e^- center-of-mass (c.m.) energy. The term including H_1^{\perp} introduces an azimuthal modulation around the direction of the fragmenting quark, called Collins asymmetry.

In $e^+e^- \rightarrow q\bar{q}$ events, the q and \bar{q} must be produced back-to-back in the e^+e^- c.m. frame with their spin aligned. For unpolarized e^+ and e^- beams at BABAR energies, the q and \bar{q} spins are polarized along either the e^+ or e^- beam direction, so there is a large transverse component when the angle between the e^+e^- and the $q\bar{q}$ axis is large. The direction is unknown for a given event, but the correlation can be exploited. Experimentally, the q and \bar{q} directions are difficult to measure, but the event thrust axis \hat{n} [21, 22] approximates at leading order the $q\bar{q}$ axis, so an azimuthal correlation between two hadrons in opposite thrust hemispheres reflects the product of the two Collins functions.

Figure 1 shows the thrust reference frame (RF12) [23]. If not otherwise specified, all kinematic variables are defined in the e^+e^- c.m. frame. The Collins effect results in a cosine modulation of the azimuthal angle $\phi_{12} = \phi_1 + \phi_2$ of the di-hadron yields. Expressing the yield as a function of ϕ_{12} (after the integration over \mathbf{P}_{hT}), and dividing by the average bin content, we obtain the normalized

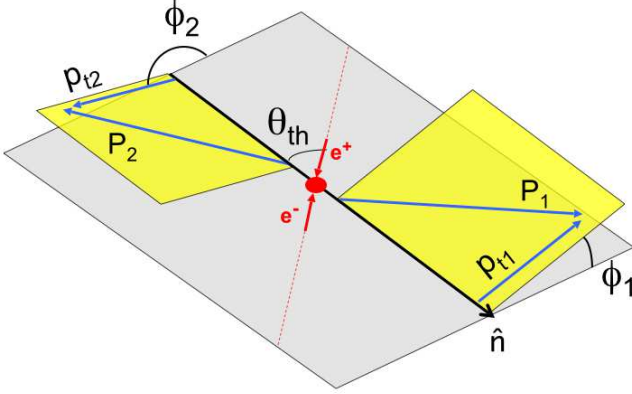


FIG. 1. (color online). Thrust reference frame (RF12). The azimuthal angles ϕ_1 and ϕ_2 are the angles between the scattering plane and the transverse hadron momenta $\mathbf{p}_{t1(t2)}$ around the thrust axis $\hat{\mathbf{n}}$. The polar angle θ_{th} is the angle between $\hat{\mathbf{n}}$ and the beam axis. Note that the difference between $\mathbf{p}_{t1(t2)}$ and \mathbf{P}_{hT} is that the latter is calculated with respect to the $q\bar{q}$ axis.

rate [11]

$$R_{12}(\phi_{12}) = 1 + \frac{\sin^2 \theta_{\text{th}}}{1 + \cos^2 \theta_{\text{th}}} \cos \phi_{12} \cdot \frac{H_1^{\perp[1]}(z_1) \overline{H}_1^{\perp[1]}(z_2)}{D_1^{[0]}(z_1) \overline{D}_1^{[0]}(z_2)}, \quad (2)$$

where the sum over the involved quark flavors is implied, θ_{th} is defined in Fig. 1, $z_{1(2)}$ is the fractional energy of the first (second) hadron, and the bar denotes the function for the \bar{q} . Equation (2) involves only the moments of FF, which are defined as

$$F^{[n]}(z_i) \equiv \int d|\mathbf{k}_{\mathbf{T}}|^2 \left[\frac{|\mathbf{k}_{\mathbf{T}}|}{M_i} \right]^n F(z_i, |\mathbf{k}_{\mathbf{T}}|^2), \quad (3)$$

with $n = 0, 1$, and $|\mathbf{k}_{\mathbf{T}}|$ the transverse momentum of the quarks with respect to the hadrons they fragment into, which, in this frame, is related to the measurement of the transverse momenta of the two hadrons with respect to the thrust axis.

Despite the simple form of the R_{12} normalized rate, which involves only the product of moments of FFs, the RF12 frame comes with several downsides, among others of having to rely on Monte Carlo (MC) simulations when using the thrust axis as a proxy for the leading-order $q\bar{q}$ axis. An alternative frame is the analogue of the Gottfried-Jackson frame [23, 24] which uses the momentum of one hadron as a reference axis, and defines a single angle ϕ_0 between the plane containing the two hadron momenta and the plane defined by the beam and the reference axis. We refer to this frame as RF0 [11, 12]. The corresponding normalized yield in the e^+e^- c.m. system

is [23]

$$R_0(2\phi_0) = 1 + \frac{\sin^2 \theta_2}{1 + \cos^2 \theta_2} \cos 2\phi_0 \cdot \frac{\mathcal{F}[(2\hat{\mathbf{h}} \cdot \mathbf{k}_{\mathbf{T}} \hat{\mathbf{h}} \cdot \mathbf{p}_{\mathbf{T}} - \mathbf{k}_{\mathbf{T}} \cdot \mathbf{p}_{\mathbf{T}}) H_1^{\perp} \overline{H}_1^{\perp}]}{(M_1 M_2) \mathcal{F}[D_1 \overline{D}_1]}, \quad (4)$$

where θ_2 is the angle between the hadron used as reference and the beam axis, $\hat{\mathbf{h}}$ is the unit vector in the direction of the transverse momentum of the first hadron relative to the axis defined by the second hadron, and \mathcal{F} is used to denote the convolution integral

$$\mathcal{F}[X\overline{X}] \equiv \sum_q e_q^2 \int d^2 \mathbf{k}_{\mathbf{T}} d^2 \mathbf{p}_{\mathbf{T}} \delta^2(\mathbf{p}_{\mathbf{T}} + \mathbf{k}_{\mathbf{T}} - \mathbf{q}_{\mathbf{T}}) X^q(z_1, z_1^2 \mathbf{k}_{\mathbf{T}}^2) \overline{X}^q(z_2, z_2^2 \mathbf{p}_{\mathbf{T}}^2), \quad (5)$$

with $\mathbf{k}_{\mathbf{T}}$, $\mathbf{p}_{\mathbf{T}}$, and $\mathbf{q}_{\mathbf{T}}$ the transverse momentum of the fragmenting quark, antiquark, and virtual photon from e^+e^- annihilation, respectively, in the frame where the two hadrons are collinear, and $X(\overline{X}) \equiv D_1(\overline{D}_1)$ or $H_1^{\perp}(\overline{H}_1^{\perp})$. In this frame, specific assumptions on the $\mathbf{k}_{\mathbf{T}}$ -dependence of the involved functions are necessary to explicitly evaluate the convolution integrals.

For this analysis we use a data sample of 468 fb^{-1} [25] collected at the c.m. energy $\sqrt{s} \approx 10.6 \text{ GeV}$ with the BABAR detector [26, 27] at the SLAC National Accelerator Laboratory. We use tracks reconstructed in the silicon vertex detector and in the drift chamber (DCH) and identified as pions or kaons in the DCH and in the Cherenkov ring imaging detector (DIRC). Detailed MC simulation is used to study detector effects and to estimate contribution from various background sources. Hadronic events are generated using the *Jetset* [28] package and undergo a full detector simulation based on GEANT4 [29].

We make a tight selection of hadronic events in order to minimize biases due to detector acceptance and hard initial-state photon radiation (ISR), as they can introduce fake azimuthal modulations. Furthermore, final-state gluon ($q\bar{q}g$) radiation also leads to angular asymmetries to be taken into account [23]. Requiring at least three charged tracks consistent with the e^+e^- primary vertex and a total visible energy of the event in the laboratory frame $E_{\text{tot}} > 11 \text{ GeV}$, we reject $e^+e^- \rightarrow \tau^+\tau^-$ and two-photon backgrounds, as well as ISR ($q\bar{q}g$) events with the photon (one jet) along the beam line. About 10% of ISR photons are within our detector acceptance, and we reject events with a photon candidate with energy above 2 GeV. We require an event thrust value $T > 0.8$ to suppress $q\bar{q}g$ and $B\bar{B}$ events, and $|\cos \theta_{\text{th}}| < 0.6$ so that most tracks are within the detector acceptance.

We assign randomly the positive direction of the thrust axis, and divide each event into two hemispheres by the plane perpendicular to it. To ensure tracks are assigned to the correct hemispheres, we require them to be within a 45° angle of the thrust axis and to have

$z > 0.15$. A “tight” identification algorithm is used to identify kaons (pions), which is about 80% (90%) efficient and has misidentification rates below 10% (5%). We select those pions and kaons that lie within the DIRC acceptance region with a polar angle in laboratory frame $0.45 \text{ rad} < \theta_{\text{lab}} < 2.46 \text{ rad}$. To minimize backgrounds, such as $e^+e^- \rightarrow \mu^+\mu^-\gamma$ followed by photon conversion, we require $z < 0.9$.

We construct all the possible pairs of selected tracks reconstructed in opposite thrust hemispheres, and we calculate the corresponding azimuthal angles ϕ_1 , ϕ_2 , and ϕ_0 in the respective reference frames. In this way, we identify three different samples of hadron pairs: KK , $K\pi$, and $\pi\pi$. To reduce low-energy gluon radiation and the contribution due to wrong hemispheres assignment, we require $Q_t < 3.5 \text{ GeV}/c$, where Q_t is the transverse momentum of the virtual photon from e^+e^- annihilation in the frame where the two hadrons are collinear [23].

The analysis is performed in intervals of hadron fractional energies with the following boundaries: 0.15, 0.2, 0.3, 0.5, 0.9, for a total of 16 two-dimensional (z_1, z_2) intervals.

For each of the three samples, we evaluate the normalized yield distributions R_{12} and R_0 for unlike (U), like (L), and any charge combination (C) of hadron pairs as a function of $\phi_1 + \phi_2$ and $2\phi_0$, as shown in the left plot of Fig. 2 for KK pairs, for example. These combinations of charged hadrons contain different contributions of favored and disfavored FFs, where a favored (disfavored) process refers to the production of a hadron for which one (none) of the valence quarks is of the same kind as the fragmenting quark. In particular, by selecting KK pairs, we are able to study the favored contribution $H_s^{\perp \text{fav}}$ of the strange quark, not accessible when considering $\pi\pi$ pairs only.

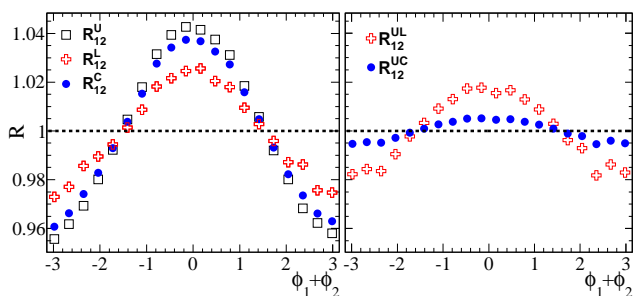


FIG. 2. (color online). Distributions of normalized yields (left plot) for unlike (U), like (L), and any charge combination (C) of KK pairs, and their double ratios (right plot) in RF12.

The normalized distributions can be parametrized with a cosine function: $R_\alpha^i = b_\alpha + a_\alpha^i \cos \beta_\alpha$, where $\alpha = 0, 12$ indicates the reference frames, $i = U, L, C$ the charge combination of hadron pairs, and $\beta_{12(0)} = \phi_{12}(2\phi_0)$.

The R_α^i distributions are strongly affected by instru-

mental effects. In order to reduce the impact of the detector acceptance, as well as any remaining effect from gluon bremsstrahlung [23], we construct two double ratios (DR) of normalized distributions, R_α^U/R_α^L and R_α^U/R_α^C . The two ratios give access to the same physical quantities as the independent R_α^i , that is the favored and disfavored FFs, but in different combinations. We report the results for both kind of DRs, which are strongly correlated since they are obtained by using the same data set. These are shown in the right plot of Fig. 2 for KK pairs in RF12. At first order, the double ratios are still parametrized by a function that is linear in the cosine of the corresponding combination of azimuthal angles:

$$R_\alpha^{ij} = \frac{R_\alpha^i}{R_\alpha^j} \simeq B_\alpha^{ij} + A_\alpha^{ij} \cdot \cos \beta_\alpha, \quad (6)$$

with B and A free parameters, and $i, j = U, L, C$. The constant term B must be consistent with unity, while A contains the information about the favored and disfavored Collins FFs.

We fit the binned R_α^{ij} distributions independently for KK , $K\pi$, and $\pi\pi$ hadron pairs. Using the MC sample, we evaluate the K/π (mis)identification probabilities for the 16 (z_1, z_2) intervals in each of the three samples. For example, the probability f_{KK}^{KK} that a true KK pair is reconstructed as KK pair is about 90% on average, slightly decreasing at higher momenta, while the probability $f_{K\pi}^{KK}$ that a true $K\pi$ pair is identified as KK is about 10%, and $f_{\pi\pi}^{KK}$ is negligible.

The presence of background processes could introduce azimuthal modulations not related to the Collins effect, and modifies the measured asymmetry as follows:

$$A_{KK}^{\text{meas}} = F_{uds}^{KK} \cdot \left(\sum_{nm} f_{nm}^{KK} \cdot A_{nm} \right) + \sum_i F_i^{KK} \left(\sum_{nm} f_{nm}^{(KK)i} \cdot A_{nm}^i \right), \quad (7)$$

with $nm = KK, K\pi, \pi\pi$, and $i = c\bar{c}, B\bar{B}, \tau^+\tau^-$. In Eq. 7, A_{nm} are the true Collins asymmetries produced from the fragmentation of light quarks in the three samples, A_{nm}^i is the i -th background asymmetry contribution, and $F_{uds(i)}^{KK}$ are the fractions of reconstructed kaon pairs coming from uds and background events, calculated from the respective MC samples. By construction, $\sum_i F_i + F_{uds} = 1$. A similar expression holds for $K\pi$ and $\pi\pi$ samples.

Previous studies [11] show that $e^+e^- \rightarrow B\bar{B}$ and $\tau^+\tau^-$ events have negligible A_{nm}^i , $F_{B\bar{B}} < 2\%$, and $F_{\tau^+\tau^-}$ significantly different from zero only for the $\pi\pi$ sample at high z values. Since $F_{c\bar{c}}$ can be as large as 30%, and $A_{c\bar{c}}$ are unknown, we determine $A_{nm}^{c\bar{c}}$ in Eq. (7) from samples enhanced in $c\bar{c}$ by requiring the reconstruction of at least one $D^{*\pm}$ meson from the decay $D^{*\pm} \rightarrow D^0\pi^\pm$, with the D^0 candidate reconstructed in the following

four Cabibbo-favored decay modes: $K^-\pi^+$, $K^-\pi^+\pi^-\pi^+$, $K_s^0\pi^+\pi^-$, and $K^-\pi^+\pi^0$. These modes are assumed to provide a representative sample of $\pi\pi$, $K\pi$, and KK pairs to be used in the correction, an assumption that is strengthened by the observation that the background asymmetries for those modes were found to be consistent. We solve the system of equations for A_{KK}^{meas} , $A_{K\pi}^{\text{meas}}$, $A_{\pi\pi}^{\text{meas}}$, for the standard and charm-enhanced samples, and we extract simultaneously the Collins asymmetries A_{KK} , $A_{K\pi}$, and $A_{\pi\pi}$, corrected for the contributions of the background and K/π (mis)identification. The dominant uncertainties related to this procedure come from the limited statistics of the D^* -enhanced sample and from the fractions F_i . The uncertainties on the fractions are evaluated by data-MC comparison and amount to a few percent. All these uncertainties are therefore included in the statistical error of the asymmetries extracted from the system of Eq. (7).

We test the DR method on the MC sample. Spin effects are not simulated in MC, and so the DR distributions should be uniform. However, when fitting the distributions for reconstructed KK pairs with Eq. (6), we measure a cosine term in the full sample of 0.004 ± 0.001 and 0.007 ± 0.001 in the RF12 and RF0 frames, respectively, indicating a bias. Smaller values are obtained for $K\pi$ and $\pi\pi$ pairs (see Fig. 5). Studies performed on the MC samples, both at generation level and after full simulation, demonstrate that the main source of this bias is due to the emission of ISR, which boosts the hadronic system and distorts the angular distribution of the final state particles, resulting in azimuthal modulations not related to the Collins effect. This effect is more pronounced for KK pairs due to the lower multiplicity with respect to the other two combinations of hadrons. Assuming the bias, which is everywhere smaller than the asymmetries measured in the data sample in each bin, is additive, we subtract it from the background-corrected asymmetry.

Using the uds MC sample, or light quark $e^+e^- \rightarrow q\bar{q}$ MC events, we study the difference between measured and true azimuthal asymmetries. The asymmetry is introduced into the simulation by reweighting the events according to the distribution $1 \pm a \cdot \cos \phi_\alpha^{\text{gen}}$, where we use different values of a ranging from 0 to 8% with positive (negative) sign for U (L and C) hadron pairs, and ϕ_α^{gen} are the azimuthal angles combinations calculated with respect to the true $q\bar{q}$ axis in RF12, or the generated hadron momentum in RF0. The reconstructed asymmetries in RF12 are systematically underestimated for the three samples of hadron pairs, as expected since we use the thrust axis instead of the $q\bar{q}$ axis, while they are consistent with the simulated ones in RF0, where only particle identification and tracking reconstruction effects could introduce possible dilution. Since we measure the same dilution for KK , $K\pi$, and $\pi\pi$ samples, the asymmetry is corrected by rescaling A_{KK} , $A_{K\pi}$, and $A_{\pi\pi}$ using the same correction factor, which ranges from 1.3

to 2.3 increasing with z , as shown in Fig. 3. No corrections are needed for the asymmetries measured in RF0. The uncertainties on the correction factors are assigned as systematic contributions.

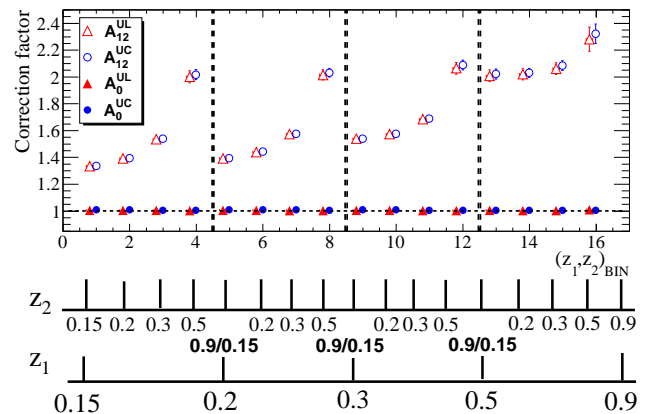


FIG. 3. (color online). Correction factors for the dilution of the asymmetry due to the difference between the thrust and the $q\bar{q}$ axis. The open (full) markers, triangles and circles, refer to the U/L and U/C double ratios in the RF12 (RF0) frame, respectively. The 16 (z_1, z_2) bins are shown on the x-axis: in each interval between the dashed lines, z_1 is chosen in the following ranges: $[0.15, 0.2]$, $[0.2, 0.3]$, $[0.3, 0.5]$, and $[0.5, 0.9]$, while within each interval the points correspond to the four bins in z_2 .

All systematic effects, if not otherwise specified, are evaluated for each bin of z . The main contribution comes from the MC bias. We compare the bias results from the nominal selection, with those obtained by requiring different cuts on E_{tot} , and/or by changing the detector acceptance region for the hadrons. The largest variation of the bias is combined in quadrature with the MC statistical error and taken as systematic uncertainty. The effects due to the particle identification are evaluated using tighter and looser selection criteria. The largest deviations with respect to the nominal selection are taken as systematic uncertainties: the average relative uncertainties are around 10%, 7%, and 5% for the KK , $K\pi$, and $\pi\pi$ pairs. Fitting the azimuthal distributions using different bin sizes, we determine relative systematic uncertainties, which are not larger than 5%, 1.9%, and 1% for the three samples. The systematic uncertainty due to the E_{tot} cut is obtained by comparing the measured asymmetries with those obtained with the looser selection $E_{\text{tot}} > 10$ GeV. The average systematic contribution is around 10% for the three samples in both reference frames. We use different fitting functions with additional higher harmonic terms. No significant changes in the value of the cosine moments with respect to the standard fits are found. As a cross-check of the double ratio method we fit the difference of R^i distributions, and we compare the two results. The difference between the

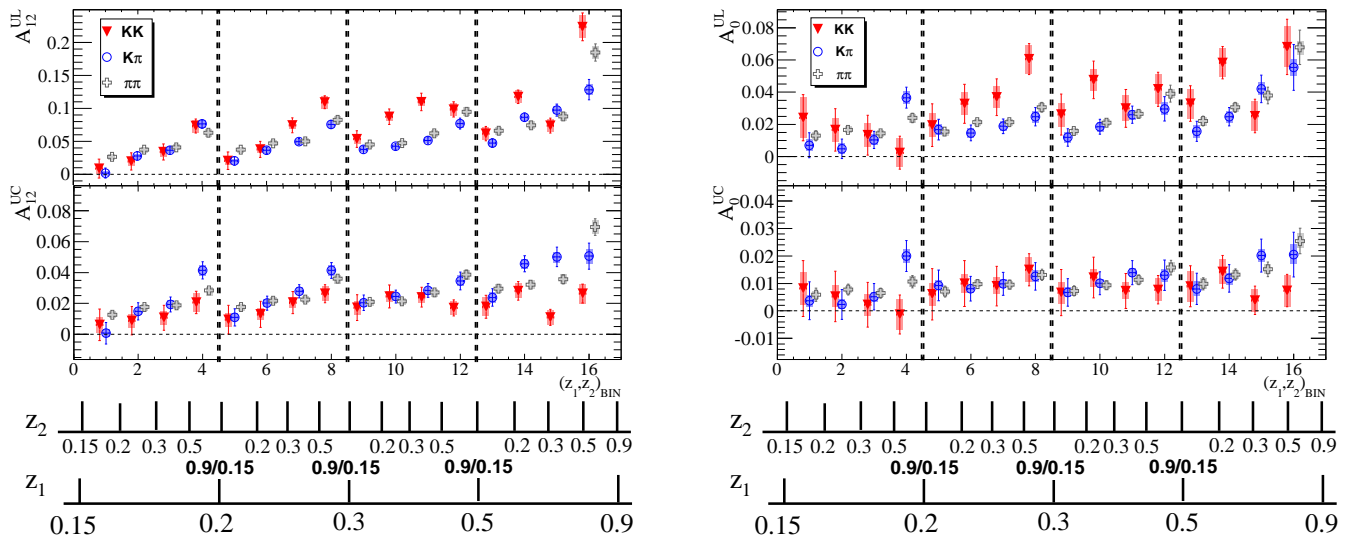


FIG. 4. (color online). Comparison of U/L (top) and U/C (bottom) Collins asymmetries in RF12 (left) and RF0 (right) for KK , $K\pi$, and $\pi\pi$ pairs. The statistical and systematic uncertainties are represented by the bars and the bands around the points, respectively. The 16 (z_1, z_2) bins are shown on the x-axis: in each interval between the dashed lines, z_1 is chosen in the following ranges: $[0.15, 0.2]$, $[0.2, 0.3]$, $[0.3, 0.5]$, and $[0.5, 0.9]$, while within each interval the points correspond to the four bins in z_2 .

two procedures is negligible for $K\pi$ and $\pi\pi$ pairs, while it reaches 1% and 3% for kaon pairs in RF12 and RF0, respectively. All the other systematic contributions are negligible [11].

The Collins asymmetries measured for the 16 two-dimensional (z_1, z_2) bins, for reconstructed KK , $K\pi$, and $\pi\pi$ hadron pairs, are shown in Fig. 4 for RF12 and RF0, and are summarized in Tables I, II, and III. The asymmetries are corrected for the background contributions and K/π contamination following Eq. (7), the MC bias is subtracted, and the corrections due to the dilution effects are applied. The total systematic uncertainties are obtained by adding in quadrature the individual contributions, and are represented by the bands around the data points.

An increasing asymmetry with increasing hadron energies is visible for the U/L double ratio in both reference frames. The largest effects, but with less precision, are observed for KK pairs, for which A_{12}^{UL} is consistent with zero at low z , and reaches 22% in the last z bin, while somewhat smaller values are seen for $\pi\pi$ and $K\pi$ pairs. In particular, at low (z_1, z_2) bins A^{UL} for $\pi\pi$ pairs is nonzero, in agreement with the behavior observed in [11]. The small differences between the two data sets are due to the different kinematic region selected after the cut on $\cos\theta_{th}$. The A^{UC} asymmetry is smaller than A^{UL} in all cases, and, for the KK pairs, the rise of the asymmetry with the hadron energies is not evident. We also note that the asymmetries for the KK pairs are larger than the others when the U/L ratio is considered, while they are at the same level, or lower, when they are extracted

from the U/C ratio.

In summary, we have studied for the first time in e^+e^- annihilation the Collins asymmetry for inclusive production of KK and $K\pi$ pairs as a function of (z_1, z_2) in two distinct reference frames. We measure the azimuthal modulation of the double ratios U/L and U/C , which are sensitive to the favored and disfavored Collins FFs for light quarks. We simultaneously extract also the Collins asymmetries for $\pi\pi$ pairs, which are found to be in agreement with those obtained in previous studies [11, 13]. The results reported in this paper and those obtained from SIDIS experiments can be used in a global analysis to extract the favored contribution of the strange quark, and to improve the knowledge on the u and d fragmentation processes [14–16].

We are grateful for the excellent luminosity and machine conditions provided by our PEP-II colleagues, and for the substantial dedicated effort from the computing organizations that support *BABAR*. The collaborating institutions wish to thank SLAC for its support and kind hospitality. This work is supported by DOE and NSF (USA), NSERC (Canada), CEA and CNRS-IN2P3 (France), BMBF and DFG (Germany), INFN (Italy), FOM (The Netherlands), NFR (Norway), MES (Russia), MEC (Spain), and STFC (United Kingdom). Individuals have received support from the Marie Curie EIF (European Union) and the A. P. Sloan Foundation.

-
- * Now at: University of Tabuk, Tabuk 71491, Saudi Arabia
 † Also at: Università di Perugia, Dipartimento di Fisica, I-06123 Perugia, Italy
 ‡ Now at: Laboratoire de Physique Nucléaire et de Hautes Energies, IN2P3/CNRS, F-75252 Paris, France
 § Now at: University of Huddersfield, Huddersfield HD1 3DH, UK
 ¶ Deceased
 ** Now at: University of South Alabama, Mobile, Alabama 36688, USA
 †† Also at: Università di Sassari, I-07100 Sassari, Italy
- [1] J. C. Collins, Nucl. Phys. B **396**, 161 (1993).
 [2] J. C. Collins and D. E. Soper, Nuclear Physics B **193**, 381 (1981).
 [3] J. Collins, D. E. Soper, and G. Sterman, Nuclear Physics B **250**, 199 (1985).
 [4] J. C. Collins and A. Metz, Phys. Rev. Lett. **93**, 252001 (2004).
 [5] P. Sun and F. Yuan, Phys. Rev. D **88**, 114012 (2013).
 [6] A. Airapetian *et al.* (The HERMES Collaboration), Phys. Rev. Lett. **94**, 012002 (2005).
 [7] A. Airapetian *et al.* (HERMES Collaboration), Phys. Lett. B **693**, 11 (2010).
 [8] C. Adolph *et al.* (COMPASS Collaboration), Phys. Lett. B **717**, 376 (2012).
 [9] M. Alekseev *et al.* (COMPASS Collaboration), Phys. Lett. B **673**, 127 (2009).
 [10] A. Airapetian *et al.* (HERMES Collaboration), Phys. Rev. D **87**, 012010 (2013).
 [11] J. Lees *et al.* (BABAR Collaboration), Phys. Rev. D **90**, 052003 (2014).
 [12] R. Seidl, G. Perdekamp, *et al.* (Belle Collaboration),

- Phys. Rev. D **78**, 032011 (2008).
 [13] R. Seidl, G. Perdekamp, *et al.* (Belle Collaboration), Phys. Rev. D **86**, 039905(E) (2012).
 [14] A. Bacchetta, L. P. Gamberg, G. R. Goldstein, and A. Mukherjee, Phys. Lett. B **659**, 234 (2008).
 [15] M. Anselmino, M. Boglione, U. D'Alesio, A. Kotzinian, F. Murgia, A. Prokudin, and C. Türk, Phys. Rev. D **75**, 054032 (2007).
 [16] M. Anselmino, M. Boglione, U. D'Alesio, S. Melis, F. Murgia, and A. Prokudin, Phys. Rev. D **87**, 094019 (2013).
 [17] R. L. Jaffe and X. Ji, Phys. Rev. Lett. **67**, 552 (1991).
 [18] J. Soffer, Phys. Rev. Lett. **74**, 1292 (1995).
 [19] A. Martin, F. Bradamante, and V. Barone, Phys. Rev. D **91**, 014034 (2015).
 [20] A. Bacchetta, U. D'Alesio, M. Diehl, and C. A. Miller, Phys. Rev. D **70**, 117504 (2004).
 [21] E. Farhi, Phys. Rev. Lett. **39**, 1587 (1977).
 [22] S. Brandt, C. Peyrou, R. Sosnowski, and A. Wroblewski, Phys. Lett. **12**, 57 (1964).
 [23] D. Boer, Nucl. Phys. B **806**, 23 (2009).
 [24] D. Boer, R. Jakob, and P. Mulders, Nuclear Physics B **504**, 345 (1997).
 [25] J. P. Lees *et al.* (BABAR Collaboration), Nucl. Instrum. Meth. A **726**, 203 (2013).
 [26] B. Aubert *et al.* (BABAR Collaboration), Nucl. Instrum. and Meth. A **479**, 1 (2002).
 [27] B. Aubert *et al.* (BABAR Collaboration), Nucl. Instrum. and Meth. A **729**, 615 (2013).
 [28] T. Sjöstrand, "PYTHIA 5.7 and JETSET 7.4: Physics and manual," (1995), arXiv:hep-ph/9508391 [hep-ph].
 [29] S. Agostinelli *et al.* (GEANT4), Nucl. Instrum. Meth. A **506**, 250 (2003).

<i>KK</i> sample						
z_1	$\langle z_1 \rangle$	z_2	$\langle z_2 \rangle$	$\frac{\langle \sin^2 \theta_{th} \rangle}{\langle 1 + \cos^2 \theta_{th} \rangle}$	$A_{12}^{UL} (10^{-2})$	$A_{12}^{UC} (10^{-2})$
[0.15, 0.2]	0.175	[0.15, 0.2]	0.175	0.797	$0.88 \pm 1.43 \pm 0.73$	$0.62 \pm 1.02 \pm 0.51$
[0.15, 0.2]	0.175	[0.2, 0.3]	0.247	0.794	$1.96 \pm 1.32 \pm 0.67$	$0.88 \pm 0.92 \pm 0.43$
[0.15, 0.2]	0.175	[0.3, 0.5]	0.381	0.794	$3.38 \pm 1.23 \pm 0.73$	$1.08 \pm 0.81 \pm 0.43$
[0.15, 0.2]	0.175	[0.5, 0.9]	0.608	0.786	$7.32 \pm 1.06 \pm 0.97$	$2.06 \pm 0.72 \pm 0.59$
[0.2, 0.3]	0.246	[0.15, 0.2]	0.175	0.794	$2.06 \pm 1.33 \pm 0.68$	$0.95 \pm 0.93 \pm 0.44$
[0.2, 0.3]	0.247	[0.2, 0.3]	0.247	0.792	$3.78 \pm 1.22 \pm 0.58$	$1.30 \pm 0.84 \pm 0.36$
[0.2, 0.3]	0.247	[0.3, 0.5]	0.382	0.792	$7.44 \pm 1.14 \pm 0.59$	$2.06 \pm 0.72 \pm 0.35$
[0.2, 0.3]	0.247	[0.5, 0.9]	0.608	0.783	$10.91 \pm 0.98 \pm 0.91$	$2.63 \pm 0.58 \pm 0.48$
[0.3, 0.5]	0.381	[0.15, 0.2]	0.175	0.794	$5.34 \pm 1.28 \pm 0.74$	$1.73 \pm 0.84 \pm 0.44$
[0.3, 0.5]	0.381	[0.2, 0.3]	0.247	0.792	$8.74 \pm 1.17 \pm 0.59$	$2.45 \pm 0.74 \pm 0.35$
[0.3, 0.5]	0.382	[0.3, 0.5]	0.382	0.792	$10.97 \pm 1.31 \pm 0.63$	$2.41 \pm 0.65 \pm 0.34$
[0.3, 0.5]	0.383	[0.5, 0.9]	0.610	0.784	$9.84 \pm 1.16 \pm 0.92$	$1.71 \pm 0.52 \pm 0.45$
[0.5, 0.9]	0.609	[0.15, 0.2]	0.175	0.785	$6.15 \pm 1.09 \pm 0.98$	$1.78 \pm 0.74 \pm 0.60$
[0.5, 0.9]	0.608	[0.2, 0.3]	0.248	0.783	$11.75 \pm 1.03 \pm 0.91$	$2.81 \pm 0.60 \pm 0.48$
[0.5, 0.9]	0.610	[0.3, 0.5]	0.383	0.784	$7.40 \pm 1.13 \pm 0.91$	$1.11 \pm 0.52 \pm 0.45$
[0.5, 0.9]	0.615	[0.5, 0.9]	0.615	0.776	$22.36 \pm 2.09 \pm 1.69$	$2.63 \pm 0.61 \pm 0.62$
z_1	$\langle z_1 \rangle$	z_2	$\langle z_2 \rangle$	$\frac{\langle \sin^2 \theta_2 \rangle}{\langle 1 + \cos^2 \theta_2 \rangle}$	$A_0^{UL} (10^{-2})$	$A_0^{UC} (10^{-2})$
[0.15, 0.2]	0.175	[0.15, 0.2]	0.175	0.739	$2.41 \pm 1.44 \pm 1.25$	$0.82 \pm 1.02 \pm 0.58$
[0.15, 0.2]	0.175	[0.2, 0.3]	0.247	0.736	$1.66 \pm 1.31 \pm 0.74$	$0.53 \pm 0.92 \pm 0.40$
[0.15, 0.2]	0.175	[0.3, 0.5]	0.381	0.750	$1.33 \pm 1.24 \pm 0.71$	$0.23 \pm 0.81 \pm 0.39$
[0.15, 0.2]	0.175	[0.5, 0.9]	0.608	0.751	$0.24 \pm 1.02 \pm 0.90$	$-0.13 \pm 0.71 \pm 0.55$
[0.2, 0.3]	0.246	[0.15, 0.2]	0.175	0.739	$1.95 \pm 1.32 \pm 0.75$	$0.61 \pm 0.93 \pm 0.41$
[0.2, 0.3]	0.247	[0.2, 0.3]	0.247	0.736	$3.28 \pm 1.21 \pm 0.69$	$1.00 \pm 0.84 \pm 0.33$
[0.2, 0.3]	0.247	[0.3, 0.5]	0.382	0.749	$3.69 \pm 1.14 \pm 0.67$	$0.90 \pm 0.72 \pm 0.31$
[0.2, 0.3]	0.247	[0.5, 0.9]	0.608	0.750	$6.05 \pm 0.96 \pm 0.88$	$1.49 \pm 0.58 \pm 0.44$
[0.3, 0.5]	0.381	[0.15, 0.2]	0.175	0.738	$2.62 \pm 1.27 \pm 0.72$	$0.67 \pm 0.84 \pm 0.39$
[0.3, 0.5]	0.381	[0.2, 0.3]	0.247	0.736	$4.76 \pm 1.17 \pm 0.67$	$1.21 \pm 0.74 \pm 0.31$
[0.3, 0.5]	0.382	[0.3, 0.5]	0.382	0.749	$2.99 \pm 1.18 \pm 0.78$	$0.73 \pm 0.63 \pm 0.31$
[0.3, 0.5]	0.383	[0.5, 0.9]	0.610	0.750	$4.18 \pm 1.06 \pm 0.92$	$0.77 \pm 0.52 \pm 0.41$
[0.5, 0.9]	0.609	[0.15, 0.2]	0.175	0.731	$3.30 \pm 1.10 \pm 0.91$	$0.90 \pm 0.74 \pm 0.56$
[0.5, 0.9]	0.608	[0.2, 0.3]	0.248	0.728	$5.83 \pm 1.00 \pm 0.88$	$1.42 \pm 0.60 \pm 0.44$
[0.5, 0.9]	0.610	[0.3, 0.5]	0.383	0.743	$2.52 \pm 1.04 \pm 0.92$	$0.38 \pm 0.51 \pm 0.41$
[0.5, 0.9]	0.615	[0.5, 0.9]	0.615	0.743	$6.81 \pm 1.72 \pm 1.26$	$0.74 \pm 0.59 \pm 0.57$

TABLE I. Light quark (*uds*) Collins asymmetries obtained by fitting the U/L and U/C double ratios as a function of (z_1, z_2) for kaon pairs in the RF12 frame (upper table) and in the RF0 frame (lower table). In the first two columns are reported the z bins and their respective mean values for the kaon in one hemisphere; in the following two columns, the same variables for the second kaon are shown; in the fifth column is summarized the ratio of mean values $\langle \sin^2 \theta_{th(2)} \rangle / \langle 1 + \cos^2 \theta_{th(2)} \rangle$, and the asymmetry results are reported in the last two columns. The quoted errors are statistical and systematic, respectively. The mean values of the quantities reported in the table are calculated by summing the corresponding values for each *KK* pair and dividing by the number of *KK* pairs that fall into each (z_1, z_2) interval. Note that the A^{UL} and A^{UC} results are strongly correlated since they are obtained by using the same data set.

$K\pi$ sample						
z_1	$\langle z_1 \rangle$	z_2	$\langle z_2 \rangle$	$\frac{\langle \sin^2 \theta_{th} \rangle}{\langle 1 + \cos^2 \theta_{th} \rangle}$	$A_{12}^{UL} (10^{-2})$	$A_{12}^{UC} (10^{-2})$
[0.15, 0.2]	0.174	[0.15, 0.2]	0.174	0.794	$0.19 \pm 0.77 \pm 0.37$	$0.07 \pm 0.69 \pm 0.25$
[0.15, 0.2]	0.174	[0.2, 0.3]	0.246	0.792	$2.73 \pm 0.62 \pm 0.36$	$1.49 \pm 0.55 \pm 0.23$
[0.15, 0.2]	0.174	[0.3, 0.5]	0.380	0.791	$3.64 \pm 0.53 \pm 0.39$	$1.93 \pm 0.48 \pm 0.24$
[0.15, 0.2]	0.174	[0.5, 0.9]	0.612	0.784	$7.63 \pm 0.64 \pm 0.56$	$4.12 \pm 0.56 \pm 0.35$
[0.2, 0.3]	0.246	[0.15, 0.2]	0.174	0.791	$2.02 \pm 0.63 \pm 0.36$	$1.10 \pm 0.56 \pm 0.23$
[0.2, 0.3]	0.245	[0.2, 0.3]	0.246	0.790	$3.64 \pm 0.50 \pm 0.38$	$2.02 \pm 0.45 \pm 0.23$
[0.2, 0.3]	0.245	[0.3, 0.5]	0.380	0.789	$4.94 \pm 0.47 \pm 0.39$	$2.79 \pm 0.42 \pm 0.24$
[0.2, 0.3]	0.245	[0.5, 0.9]	0.611	0.782	$7.56 \pm 0.61 \pm 0.52$	$4.13 \pm 0.52 \pm 0.32$
[0.3, 0.5]	0.380	[0.15, 0.2]	0.174	0.791	$3.76 \pm 0.55 \pm 0.39$	$2.04 \pm 0.50 \pm 0.25$
[0.3, 0.5]	0.380	[0.2, 0.3]	0.245	0.789	$4.24 \pm 0.47 \pm 0.39$	$2.44 \pm 0.42 \pm 0.24$
[0.3, 0.5]	0.379	[0.3, 0.5]	0.379	0.788	$5.14 \pm 0.54 \pm 0.41$	$2.84 \pm 0.45 \pm 0.25$
[0.3, 0.5]	0.379	[0.5, 0.9]	0.612	0.781	$7.70 \pm 0.82 \pm 0.56$	$3.46 \pm 0.57 \pm 0.34$
[0.5, 0.9]	0.612	[0.15, 0.2]	0.174	0.784	$4.75 \pm 0.63 \pm 0.55$	$2.39 \pm 0.57 \pm 0.35$
[0.5, 0.9]	0.611	[0.2, 0.3]	0.245	0.782	$8.65 \pm 0.63 \pm 0.52$	$4.57 \pm 0.52 \pm 0.32$
[0.5, 0.9]	0.612	[0.3, 0.5]	0.379	0.781	$9.74 \pm 0.92 \pm 0.57$	$5.01 \pm 0.63 \pm 0.34$
[0.5, 0.9]	0.615	[0.5, 0.9]	0.615	0.777	$12.83 \pm 1.54 \pm 0.81$	$5.06 \pm 0.85 \pm 0.46$
z_1	$\langle z_1 \rangle$	z_2	$\langle z_2 \rangle$	$\frac{\langle \sin^2 \theta_2 \rangle}{\langle 1 + \cos^2 \theta_2 \rangle}$	$A_0^{UL} (10^{-2})$	$A_0^{UC} (10^{-2})$
[0.15, 0.2]	0.174	[0.15, 0.2]	0.174	0.732	$0.70 \pm 0.78 \pm 0.36$	$0.37 \pm 0.69 \pm 0.21$
[0.15, 0.2]	0.174	[0.2, 0.3]	0.246	0.736	$0.48 \pm 0.61 \pm 0.32$	$0.23 \pm 0.55 \pm 0.17$
[0.15, 0.2]	0.174	[0.3, 0.5]	0.380	0.748	$1.04 \pm 0.53 \pm 0.31$	$0.52 \pm 0.48 \pm 0.17$
[0.15, 0.2]	0.174	[0.5, 0.9]	0.612	0.752	$3.66 \pm 0.64 \pm 0.39$	$2.00 \pm 0.56 \pm 0.25$
[0.2, 0.3]	0.246	[0.15, 0.2]	0.174	0.727	$1.68 \pm 0.63 \pm 0.32$	$0.93 \pm 0.56 \pm 0.17$
[0.2, 0.3]	0.245	[0.2, 0.3]	0.246	0.733	$1.47 \pm 0.50 \pm 0.29$	$0.79 \pm 0.45 \pm 0.14$
[0.2, 0.3]	0.245	[0.3, 0.5]	0.380	0.746	$1.89 \pm 0.46 \pm 0.31$	$0.98 \pm 0.42 \pm 0.15$
[0.2, 0.3]	0.245	[0.5, 0.9]	0.611	0.750	$2.47 \pm 0.57 \pm 0.35$	$1.26 \pm 0.50 \pm 0.21$
[0.3, 0.5]	0.380	[0.15, 0.2]	0.174	0.724	$1.19 \pm 0.55 \pm 0.31$	$0.67 \pm 0.50 \pm 0.17$
[0.3, 0.5]	0.380	[0.2, 0.3]	0.245	0.731	$1.86 \pm 0.46 \pm 0.31$	$1.01 \pm 0.42 \pm 0.15$
[0.3, 0.5]	0.379	[0.3, 0.5]	0.379	0.744	$2.60 \pm 0.53 \pm 0.30$	$1.39 \pm 0.44 \pm 0.15$
[0.3, 0.5]	0.379	[0.5, 0.9]	0.612	0.749	$2.96 \pm 0.75 \pm 0.37$	$1.30 \pm 0.56 \pm 0.22$
[0.5, 0.9]	0.612	[0.15, 0.2]	0.174	0.717	$1.57 \pm 0.63 \pm 0.39$	$0.80 \pm 0.57 \pm 0.26$
[0.5, 0.9]	0.611	[0.2, 0.3]	0.245	0.725	$2.48 \pm 0.57 \pm 0.35$	$1.18 \pm 0.50 \pm 0.21$
[0.5, 0.9]	0.612	[0.3, 0.5]	0.379	0.738	$4.20 \pm 0.86 \pm 0.37$	$2.01 \pm 0.60 \pm 0.23$
[0.5, 0.9]	0.615	[0.5, 0.9]	0.615	0.745	$5.53 \pm 1.43 \pm 0.52$	$2.05 \pm 0.81 \pm 0.35$

TABLE II. Light quark (uds) Collins asymmetries obtained by fitting the U/L and U/C double ratios as a function of (z_1, z_2) for $K\pi$ hadron pairs in the RF12 frame (upper table) and in the RF0 frame (lower table). In the first two columns are reported the z bins and their respective mean values for the hadron (K or π) in one hemisphere; in the following two columns, the same variables for the second hadron (K or π) are shown; in the fifth column is summarized the ratio of mean values $\langle \sin^2 \theta_{th(2)} \rangle / \langle 1 + \cos^2 \theta_{th(2)} \rangle$, and the asymmetry results are reported in the last two columns. The quoted errors are statistical and systematic, respectively. The mean values of the quantities reported in the table are calculated by summing the corresponding values for each $K\pi$ pair and dividing by the number of $K\pi$ pairs that fall into each (z_1, z_2) interval. Note that the A^{UL} and A^{UC} results are strongly correlated since they are obtained by using the same data set.

$\pi\pi$ sample						
z_1	$\langle z_1 \rangle$	z_2	$\langle z_2 \rangle$	$\frac{\langle \sin^2 \theta_{th} \rangle}{\langle 1 + \cos^2 \theta_{th} \rangle}$	$A_{12}^{UL} (10^{-2})$	$A_{12}^{UC} (10^{-2})$
[0.15, 0.2]	0.174	[0.15, 0.2]	0.174	0.791	$2.64 \pm 0.37 \pm 0.39$	$1.25 \pm 0.26 \pm 0.20$
[0.15, 0.2]	0.174	[0.2, 0.3]	0.244	0.789	$3.72 \pm 0.29 \pm 0.40$	$1.74 \pm 0.21 \pm 0.19$
[0.15, 0.2]	0.174	[0.3, 0.5]	0.378	0.786	$4.06 \pm 0.24 \pm 0.43$	$1.87 \pm 0.19 \pm 0.21$
[0.15, 0.2]	0.174	[0.5, 0.9]	0.617	0.781	$6.26 \pm 0.34 \pm 0.57$	$2.80 \pm 0.23 \pm 0.29$
[0.2, 0.3]	0.244	[0.15, 0.2]	0.174	0.789	$3.76 \pm 0.29 \pm 0.40$	$1.76 \pm 0.21 \pm 0.19$
[0.2, 0.3]	0.244	[0.2, 0.3]	0.244	0.788	$4.69 \pm 0.21 \pm 0.41$	$2.17 \pm 0.17 \pm 0.20$
[0.2, 0.3]	0.244	[0.3, 0.5]	0.377	0.785	$4.99 \pm 0.21 \pm 0.44$	$2.24 \pm 0.16 \pm 0.21$
[0.2, 0.3]	0.244	[0.5, 0.9]	0.617	0.780	$8.27 \pm 0.36 \pm 0.58$	$3.57 \pm 0.22 \pm 0.28$
[0.3, 0.5]	0.378	[0.15, 0.2]	0.174	0.786	$4.53 \pm 0.25 \pm 0.43$	$2.08 \pm 0.19 \pm 0.21$
[0.3, 0.5]	0.377	[0.2, 0.3]	0.244	0.785	$4.73 \pm 0.21 \pm 0.44$	$2.12 \pm 0.16 \pm 0.21$
[0.3, 0.5]	0.377	[0.3, 0.5]	0.377	0.782	$6.23 \pm 0.33 \pm 0.48$	$2.70 \pm 0.19 \pm 0.23$
[0.3, 0.5]	0.378	[0.5, 0.9]	0.619	0.777	$9.47 \pm 0.59 \pm 0.62$	$3.85 \pm 0.29 \pm 0.30$
[0.5, 0.9]	0.617	[0.15, 0.2]	0.174	0.781	$6.58 \pm 0.37 \pm 0.58$	$2.94 \pm 0.24 \pm 0.29$
[0.5, 0.9]	0.617	[0.2, 0.3]	0.244	0.780	$7.45 \pm 0.35 \pm 0.58$	$3.21 \pm 0.22 \pm 0.28$
[0.5, 0.9]	0.619	[0.3, 0.5]	0.378	0.777	$8.77 \pm 0.59 \pm 0.62$	$3.55 \pm 0.29 \pm 0.30$
[0.5, 0.9]	0.622	[0.5, 0.9]	0.622	0.772	$18.46 \pm 1.31 \pm 0.98$	$6.93 \pm 0.54 \pm 0.43$
z_1	$\langle z_1 \rangle$	z_2	$\langle z_2 \rangle$	$\frac{\langle \sin^2 \theta_2 \rangle}{\langle 1 + \cos^2 \theta_2 \rangle}$	$A_0^{UL} (10^{-2})$	$A_0^{UC} (10^{-2})$
[0.15, 0.2]	0.174	[0.15, 0.2]	0.174	0.725	$1.26 \pm 0.31 \pm 0.22$	$0.59 \pm 0.24 \pm 0.14$
[0.15, 0.2]	0.174	[0.2, 0.3]	0.244	0.735	$1.66 \pm 0.25 \pm 0.21$	$0.78 \pm 0.20 \pm 0.13$
[0.15, 0.2]	0.174	[0.3, 0.5]	0.378	0.744	$1.41 \pm 0.22 \pm 0.22$	$0.65 \pm 0.18 \pm 0.13$
[0.15, 0.2]	0.174	[0.5, 0.9]	0.617	0.750	$2.39 \pm 0.30 \pm 0.27$	$1.05 \pm 0.22 \pm 0.18$
[0.2, 0.3]	0.244	[0.15, 0.2]	0.174	0.722	$1.52 \pm 0.25 \pm 0.21$	$0.71 \pm 0.20 \pm 0.13$
[0.2, 0.3]	0.244	[0.2, 0.3]	0.244	0.733	$2.12 \pm 0.20 \pm 0.21$	$0.98 \pm 0.16 \pm 0.12$
[0.2, 0.3]	0.244	[0.3, 0.5]	0.377	0.742	$2.13 \pm 0.20 \pm 0.21$	$0.96 \pm 0.16 \pm 0.13$
[0.2, 0.3]	0.244	[0.5, 0.9]	0.617	0.748	$3.03 \pm 0.30 \pm 0.25$	$1.31 \pm 0.20 \pm 0.16$
[0.3, 0.5]	0.378	[0.15, 0.2]	0.174	0.718	$1.58 \pm 0.23 \pm 0.22$	$0.73 \pm 0.18 \pm 0.13$
[0.3, 0.5]	0.377	[0.2, 0.3]	0.244	0.729	$2.09 \pm 0.20 \pm 0.21$	$0.93 \pm 0.16 \pm 0.13$
[0.3, 0.5]	0.377	[0.3, 0.5]	0.377	0.738	$2.64 \pm 0.27 \pm 0.22$	$1.13 \pm 0.17 \pm 0.13$
[0.3, 0.5]	0.378	[0.5, 0.9]	0.619	0.746	$3.89 \pm 0.52 \pm 0.28$	$1.58 \pm 0.27 \pm 0.18$
[0.5, 0.9]	0.617	[0.15, 0.2]	0.174	0.712	$2.20 \pm 0.30 \pm 0.27$	$0.98 \pm 0.22 \pm 0.18$
[0.5, 0.9]	0.617	[0.2, 0.3]	0.244	0.724	$3.06 \pm 0.31 \pm 0.25$	$1.32 \pm 0.21 \pm 0.16$
[0.5, 0.9]	0.619	[0.3, 0.5]	0.378	0.735	$3.76 \pm 0.51 \pm 0.28$	$1.52 \pm 0.27 \pm 0.18$
[0.5, 0.9]	0.622	[0.5, 0.9]	0.622	0.743	$6.76 \pm 1.06 \pm 0.41$	$2.54 \pm 0.46 \pm 0.26$

TABLE III. Light quark (uds) Collins asymmetries obtained by fitting the U/L and U/C double ratios as a function of (z_1, z_2) for kaon pairs in the RF12 frame (upper table) and in the RF0 frame (lower table). In the first two columns are reported the z bins and their respective mean values for the kaon in one hemisphere; in the following two columns, the same variables for the second kaon are shown; in the fifth column is summarized the ratio of mean values $\langle \sin^2 \theta_{th(2)} \rangle / \langle 1 + \cos^2 \theta_{th(2)} \rangle$, and the asymmetry results are reported in the last two columns. The quoted errors are statistical and systematic, respectively. The mean values of the quantities reported in the table are calculated by summing the corresponding values for each $\pi\pi$ pair and dividing by the number of $\pi\pi$ pairs that fall into each (z_1, z_2) interval. Note that the A^{UL} and A^{UC} results are strongly correlated since they are obtained by using the same data set.

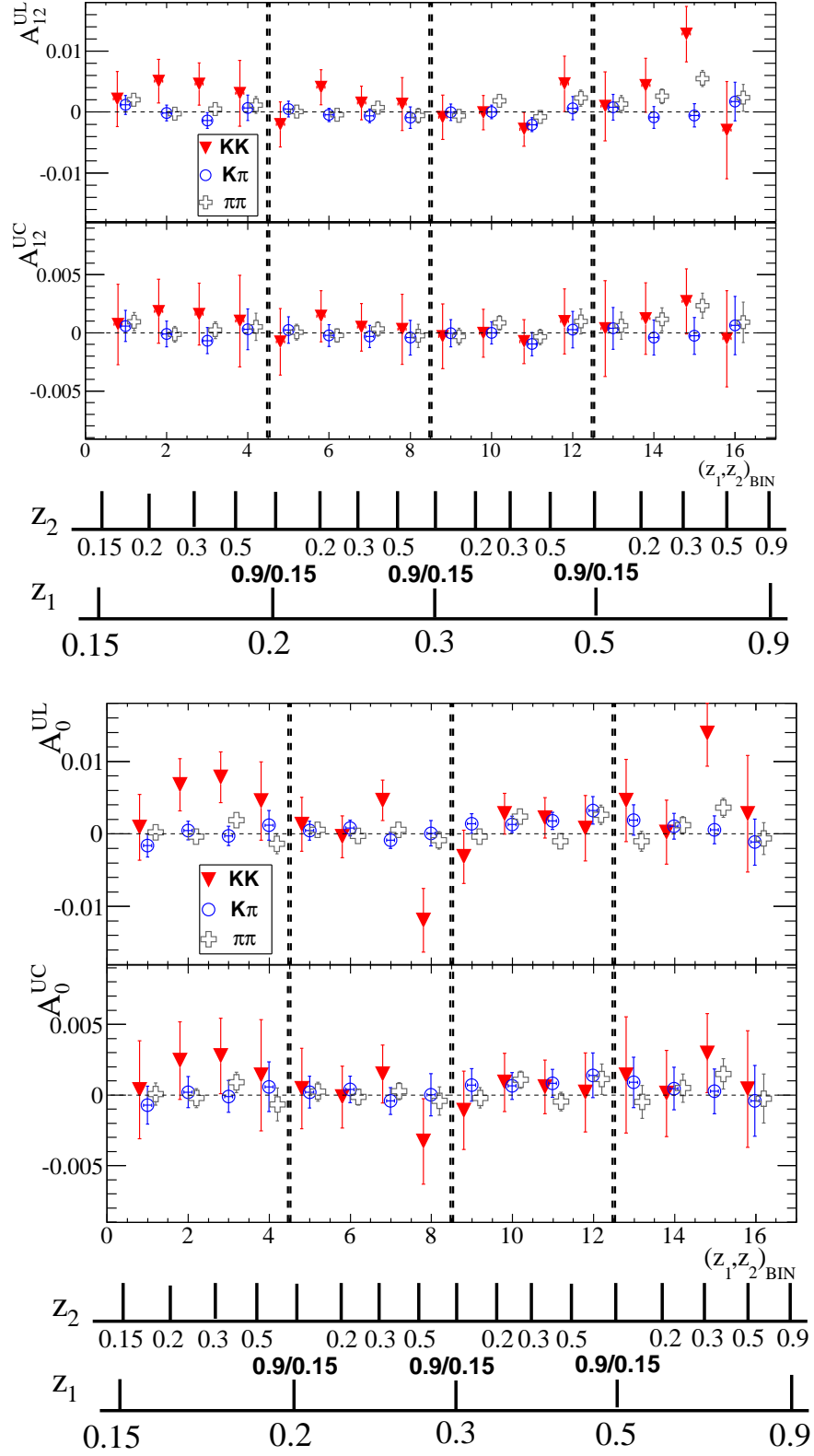


FIG. 5. (color online). Asymmetries measured in the MC sample in RF12 (top) and RF0 (bottom) for KK , $K\pi$, and $\pi\pi$ pairs. The upper plots show the U/L double ratio, while the lower plots the U/C double ratio. The 16 (z_1, z_2) bins are shown on the x-axis: in each interval between the dashed lines, z_1 is chosen in the following ranges: $[0.15, 0.2]$, $[0.2, 0.3]$, $[0.3, 0.5]$, and $[0.5, 0.9]$, while within each interval the points correspond to the four bins in z_2 . We subtract these biases from the background-corrected asymmetry, and the statistical errors (represented by the bars around the points) are included into the systematic uncertainties.